A LINEAR-TIME-VARYING APPROACH FOR EXACT IDENTIFICATION OF BILINEAR DISCRETE-TIME SYSTEMS BY INTERACTION MATRICES

Francesco Vicario,[*] **Minh Q. Phan,**[†]
Richard W. Longman,[‡] **and Raimondo Betti**[§]

Bilinear systems offer a promising approach for nonlinear control because a broad class of nonlinear problems can be reformulated in bilinear form. In this paper system identification is shown to be a technique to obtain such a bilinear approximation of a nonlinear system. Recent discrete-time bilinear model identification methods rely on Input-Output-to-State Representations. These IOSRs are exact only for a certain class of bilinear systems, and they are also limited by high dimensionality and explicit bounds on the input magnitude. This paper offers new IOSRs where the bilinear system is treated as a linear time-varying system through the use of specialized input signals. All the mentioned limitations are overcome by the new approach, leading to more accurate and less computationally demanding identification methods for bilinear discrete-time models, which are also shown via examples to be applicable to the identification of bilinear models approximating more general nonlinear systems.

INTRODUCTION

Bilinear systems have the property that they are linear in the state variables if the input is held constant and are also linear in the input if the state is held constant. In other words, the nonlinearity in bilinear systems is due to the presence of products between the state and the input. Bilinear models are important per se since several phenomena in engineering (in particular chemical processes), biology, physiology, sociology and other fields (Reference 1) are inherently bilinear. More interestingly, by increasing the state dimension a bilinear model can be used to approximate more general nonlinear systems, namely input-affine dynamical systems (References 2, 3, 4). Interest in bilinear systems has recently grown after a technique formally known as *Carleman linearization* was found to achieve such an approximation (References 5, 6, 7). Given a specific nonlinear model, the construction of a corresponding bilinear model by Carleman linearization is a fairly complicated and tedious process. System identification can be a tool to find such a bilinear approximation in an automated fashion, by generating simulated data from the nonlinear equation and using it for identification. Even more importantly, system identification can be used to identify the bilinear model approximating the nonlinear system directly from the input-output measurements of the (unknown) nonlinear system. One can then think of bilinear system identification as a way to obtain from measured input-output data a mathematical model providing better than linear approximation to unknown nonlinear systems. At the same time, bilinear models have sufficient mathematical structure to aim to develop state estimators and control design techniques, therefore they represent a promising approach to handle nonlinear control problems such as, for example, the satellite attitude control.

[*]Doctoral Student, Department of Mechanical Engineering, Columbia University, New York, NY 10027, USA.

[†]Associate Professor, Thayer School of Engineering, Dartmouth College, Hanover, NH 03755, USA.

[‡]Professor, Department of Mechanical Engineering and Department of Civil Engineering and Engineering Mechanics, Columbia University, New York, NY 10027, USA.

[§]Professor, Department of Civil Engineering and Engineering Mechanics, Columbia University, New York, NY 10027, USA.

Although well-established techniques exist for the identification of linear systems, this is not the case for bilinear systems. Recently interaction matrices were successfully introduced in discrete-time bilinear system identification (References 8, 9). Drawing inspiration from the technique at the basis of the Observer-Kalman filter Identification (OKID) method originally developed for lightly damped linear structures and at the core of the software package distributed by NASA with title SOCIT (References 10, 11), interaction matrices were used to derive linear Input-Output-to-State Representations (IOSRs) for bilinear systems, i.e. relationships expressing the state at any time step as a linear function of a superstate defined in terms of only input-output data (typically from the p past time steps or from the p future time steps). The so derived IOSRs were then used to develop identification algorithms for bilinear systems known as Equivalent Linear Model (ELM) and Intersection Subspace (IS) methods (References 8, 9, 12). Interaction matrices giving rise to exact IOSRs exist however only for very specific bilinear models. In Reference 9 a theorem was proven ensuring the existence of interaction matrices such that the resulting IOSRs converge to exact relationships as the IOSR order p is increased. Unfortunately, the dimension of the superstate, and hence the required computational effort, increases exponentially with p. The drawback becomes more relevant when one wants to identify high-order bilinear systems, as is the case in the use of bilinear models to approximate more general nonlinear systems as mentioned above. Another drawback of the methods presented in References 8, 9 is that convergence of IOSRs as p increases is guaranteed only if the input magnitude is kept within a certain bound, which additionally is unknown before system identification is performed. This is a source of uncertainty in the choice of the input excitation for the identification and can also be a potentially severe limitation if it turns out that the bound is too small for the given application.

In this paper, a new approach is presented to derive small-dimension IOSRs which are exact for any arbitrary bilinear model and any input magnitude, overcoming the above-mentioned difficulties of previous algorithms. The new approach exploits the fact that a bilinear system can be seen as a linear-time-varying (LTV) model in state-space form whose system matrix A changes over time. Being the product of the state and the input, the additional term $Nx(k)u(k)$ characterizing bilinear systems can be lumped with the linear term $Ax(k)$ to rewrite the bilinear system as a linear model with time-varying system matrix $A + Nu(k)$. Interaction matrices are then used on the LTV formulation of a bilinear system to derive exact time-varying IOSRs of minimum order and even minimum dimension for the given order. The computational benefit is twofold. Not only is the time-varying IOSR exact with minimum order p (less than or equal to the order n of the bilinear model) but also the dimension of the corresponding superstate is increasing linearly with p instead of exponentially, making the approach very attractive when dealing with high-order bilinear models. Also, the LTV approach requires that the input takes at each time step any value from a finite set whose values must be specified a priori but are not subject to any constraint (not even on magnitude) for the algorithm to work. For the application of ELM or IS identification methods, the time-varying IOSRs need to be transformed into time-invariant IOSRs. This operation is crucial since, if performed naively, it generally leads to a fast increase in the dimension of the time-invariant IOSR. In this paper we also address this problem and show how thoughtful design of the input excitation preserves the algorithm computational efficiency obtained with the LTV approach. We provide a method to generate an input sequence which is sufficiently rich for identification and at the same time keeps under control the computational requirements of the algorithm.

All these advantages make of the proposed method a crucial step towards the realization of the above mentioned bridge between linear and nonlinear systems, where the identification of high-order bilinear models is usually expected. For the purpose of illustrating the potential of the method, detailed examples are given on (input-affine) nonlinear dynamic systems of practical interest, such as the mechanical oscillator with cubic spring, also known as Duffing's equation, and the rotation of a rigid body in a reference frame fixed to the rotating body, typically referred to as Euler's equations.

PROBLEM STATEMENT

Consider an n-state, single-input, q-output bilinear system in state-space form

$$x(k+1) = Ax(k) + Nx(k)u(k) + Bu(k) \tag{1a}$$
$$y(k) = Cx(k) + Du(k) \tag{1b}$$

A single set of length l of input-output data that starts from some unknown initial state $x(0)$ is given

$$\{u(k)\} = \{u(0), \quad u(1), \quad u(2), \quad ..., \quad u(l-1)\} \tag{2a}$$

$$\{y(k)\} = \{y(0), \quad y(1), \quad y(2), \quad ..., \quad y(l-1)\} \tag{2b}$$

The objective is to identify the system of Eq. (1) with the input-output data provided in Eq. (2). The data is assumed to be of sufficient length and richness so that the system of Eq. (1) can be correctly identified. For simplicity, we focus on the single-input case in this paper. Extension to the multi-input case can be made without conceptual difficulties and is demonstrated in this paper by an example of Euler's equations.

INPUT-OUTPUT-TO-STATE REPRESENTATIONS

Two different approaches to bilinear system identification are used in this work, namely the Equivalent Linear Model (ELM) method (References 8,9,12) and the Intersection Subspace (IS) method (Reference 9). Their detailed descriptions are given in the provided references. For the purpose of the present paper, it is sufficient to remark that at the core of both approaches is the following linear relationship between the state $x(k)$ of the bilinear system and a superstate $z(k)$ made of input-output data only

$$x(k) = Tz(k) \tag{3}$$

where T is a constant matrix. Relations of the form of Eq. (3) play a central role and are referred to as *Input-Output-to-State Representations (IOSRs)*. Defining the matrices

$$X = \begin{bmatrix} x(k_i) & x(k_i+1) & x(k_i+2) & ... & x(k_f) \end{bmatrix} \tag{4a}$$

$$Z = \begin{bmatrix} z(k_i) & z(k_i+1) & z(k_i+2) & ... & z(k_f) \end{bmatrix} \tag{4b}$$

where k_i and k_f are the initial and final time steps for which Eq. (3) holds, it is possible to write the IOSR in matrix form

$$X = TZ \tag{5}$$

Depending on the specific choice of IOSR or, equivalently, on the specific definition chosen for the superstate $z(k)$, several identification algorithms of ELM and IS type can be devised. Also notice that the implementation of the IS method requires the existence of two independent IOSRs, while for the ELM method one IOSR is sufficient.

As a note on the richness of excitation required for bilinear system identification, it is worth mentioning that it is method dependent. On top of the general conditions for bilinear system identifiability (Reference 13), the chosen identification method will add further richness requirements. Also, the adequacy of input richness can be assessed at the last step of the chosen method, when the reconstructed state history is used to build the least-squares problem whose solution yields the estimate of the matrices A, B, N, C, D. A sufficient input richness condition is that the state-input matrix to be pseudo-inverted is full-rank (Reference 9).

In Reference 9 several IOSRs were presented. The key concept behind their derivation is that of *interaction matrix* (Reference 11). The interaction matrices were originally formulated by Minh Q. Phan in the context of linear system identification of lightly-damped large flexible space structures. The interaction matrix provides a mechanism to find a compressed but equivalent dynamic representation of such structures. The compression can be exact and extremely efficient. Later development revealed that the interaction matrix in the state-space system identification problem could be interpreted as a Kalman filter gain that is optimal with respect to the system and the (unknown) process and measurement noise statistics embedded in the input-output data. This development led to the Observer/Kalman filter Identification (OKID) algorithm (Reference 10).

In this section, two of the IOSRs from Reference 9, here referred to as Time-Invariant (TI) IOSRs, are briefly reviewed and then it is shown in more details how the interaction matrices can also be applied (with a different approach with respect to Reference 9) to derive the Time-Varying (TV) IOSRs at the core of the present paper.

Time-Invariant IOSRs

For the detailed derivation and analysis of the following TI IOSRs, the reader is referred to Reference 9. Here only a brief presentation is provided, for the purpose of comparison with the TV IOSRs introduced later in this paper.

TI Causal IOSRs

A causal IOSR is here defined as a representation of the form of Eq. (3) where the state depends on past (and current, at most) input-output data only, i.e. $x(k)$ depends on $u(i)$ and $y(i)$ with $i \leq k$. In the following equations, the subscript c remarks the *causality* of the representation. By introducing two interaction matrices M'_c and M''_c, Eq. (1a) can be written as

$$x(k+1) = \bar{A}_c x(k) + \bar{N}_c x(k) u(k) + \bar{B}_c v(k) \tag{6}$$

where

$$\bar{A}_c = A + M'_c C \qquad \bar{N}_c = N + M''_c C \tag{7a}$$

$$\bar{B}_c = \begin{bmatrix} B + M'_c D & -M'_c & M''_c D & -M''_c \end{bmatrix} \qquad v_c(k) = \begin{bmatrix} u(k) \\ y(k) \\ u^2(k) \\ y(k)u(k) \end{bmatrix} \tag{7b}$$

Propagating Eq. (6) forward in time by $p-1$ steps, the following IOSR of order p is obtained

$$x(k) = T_{p,c} z_{p,c}(k) \tag{8}$$

where the superstate $z_{p,c}(k)$ is made of input-output data at steps $k-1$, $k-2$, ... , $k-p$ only. Letting $nCk = \binom{n}{k}$ denote the combinations of k out of n terms, commonly referred to as n-choose-k, the general pattern for the entries of the column vector $z_{p,c}(k+p)$ is:

- $v_c(k)$, $v_c(k+1)$, ..., $v_c(k+p-1)$

- $v_c(k)$ multiplied with products of $u(k+1)$ to $u(k+p-1)$ in all possible combinations $(p-1)C1$, $(p-1)C2$, ..., $(p-1)C(p-1)$ of $\{u(k+1), u(k+2), ..., u(k+p-1)\}$

- $v_c(k+1)$ multiplied with products of $u(k+2)$ to $u(k+p-1)$ in all possible combinations $(p-2)C1$, $(p-2)C2$, ..., $(p-2)C(p-2)$ of $\{u(k+2), u(k+3), ..., u(k+p-1)\}$
  .
  .

- $v_c(k+p-3)$ multiplied with products of $u(k+p-2)$ and $u(k+p-1)$ in all possible combinations $2C1$, $2C2$ of $\{u(k+3), u(k+4), ..., u(k+p-1)\}$

- $v_c(k+p-2)$ multiplied with $1C1$ of $u(k+p-1)$, which of course is $u(k+p-1)$

To obtain an expression for $z_{p,c}(k)$, we simply shift the time indices of $z_{p,c}(k+p)$ backwards by p time steps. For example, for $p = 2$, $T_{2,c}$ and $z_{2,c}(k)$ become

$$T_{2,c} = \begin{bmatrix} \bar{A}_c \bar{B}_c & \bar{N}_c \bar{B}_c & \bar{B}_c \end{bmatrix} \qquad z_{2,c}(k) = \begin{bmatrix} v_c(k-2) \\ v_c(k-2)u(k-1) \\ v_c(k-1) \end{bmatrix} \tag{9}$$

TI Anticausal IOSRs

An anticausal IOSR is here defined as a representation of the form of Eq. (3) where the state depends on future (and current, at most) input-output data only, i.e. $x(k)$ depends on $u(i)$ and $y(i)$ with $i \geq k$.

Rewrite Eq. (1) as

$$x(k) = A^{-1}x(k+1) - A^{-1}Nx(k)u(k) - A^{-1}Bu(k) \tag{10a}$$
$$y(k) = Cx(k) + Du(k) \tag{10b}$$

and introduce *another* pair of interaction matrices, M_a' and M_a'', where the subscript a stands for *anticausal*. Equation (10a) can then be written as

$$x(k) = \bar{A}_a x(k+1) + \bar{N}_a x(k)u(k) + \bar{B}_a v_a(k+1) \tag{11}$$

where

$$\bar{A}_a = A^{-1} + M_a'C \qquad \bar{N}_a = -A^{-1}N + M_a''C \tag{12a}$$

$$\bar{B}_a = -\begin{bmatrix} A^{-1}B & -M_a'D & M_a' & -M_a''D & M_a'' \end{bmatrix} \qquad v_a(k+1) = \begin{bmatrix} u(k) \\ u(k+1) \\ y(k+1) \\ u^2(k) \\ y(k)u(k) \end{bmatrix} \tag{12b}$$

The resulting anticausal IOSR of order p is denoted by

$$x(k) = T_{p,a} z_{p,a}(k) \tag{13}$$

where the superstate $z_{p,a}(k)$ is defined as the column vector with the following entries

- $v_a(k+1)u^i(k)$ for all $i = 0, 1, ..., p-1$
- $v_a(k+2)u^{i_1}(k)u^{i_2}(k+1)$ for all $i_1, i_2 \geq 0$ and $i_1 + i_2 \leq p-2$
  .
  .
- $v_a(k+r)u^{i_1}(k)u^{i_2}(k+1)...u^{i_p}(k+p-r)$ for all $i_j \geq 0$ and $\sum_{j=1}^r i_j \leq p-r$
  .
  .
- $v_a(k+p)$

and depends on input-output data at steps $k, k+1, ... , k+p$ only. For example, for $p = 2$, $T_{2,a}$ and $z_{2,a}(k)$ become

$$T_{2,a} = \begin{bmatrix} \bar{A}_a\bar{B}_a & \bar{N}_a\bar{B}_a & \bar{B}_a \end{bmatrix} \qquad z_{2,a}(k) = \begin{bmatrix} v_a(k+2) \\ v_a(k+1)u(k) \\ v_a(k+1) \end{bmatrix} \tag{14}$$

Note that the above definition of superstate $z_{p,a}(k)$ with $v_a(k)$ given by Eq. (12b) leads to some redundancy in the entries of $z_{p,a}(k)$, which is suggested to be eliminated when implementing the desired identification algorithm.

Drawbacks of the TI IOSRs

The two main drawbacks of the TI IOSRs are their approximate nature and the exponential growth in dimension as their order p is increased to reduce the approximation error.

The conditions for the TI IOSRs, Eqs. (8) and (13), to be exact relationships are indeed very restrictive. For the causal IOSR, it is necessary that all the possible products of overall power p of matrices $\bar{A}_c$ and $\bar{N}_c$ are zero, which in this paper is more compactly indicated as

$$\mathcal{C}_p\big(\bar{A}_c, \bar{N}_c\big) = 0 \tag{15}$$

For instance, for a causal IOSR of order $p = 2$, the condition of Eq. (15) becomes

$$\bar{A}_c^2 = \bar{A}_c\bar{N}_c = \bar{N}_c\bar{A}_c = \bar{N}_c^2 = 0 \tag{16}$$

Similarly, for the anticausal IOSR, it is necessary that

$$\mathcal{C}_p\big(\bar{A}_a, \bar{N}_a\big) = 0 \tag{17}$$

Bilinear systems satisfying either of the above conditions for some p are referred to as *ideal* in *forward* or *backward* sense, respectively. In practice, ideal bilinear systems are rare. However, in Reference 9 a theorem was proven ensuring that there exist interaction matrices to make the above IOSRs asymptotically exact for any bilinear system, i.e. the TI IOSRs converge to exact relationships as p is increased. Additionally, the convergence is ensured only if the excitation input magnitude is bound by a value γ, which is unknown before the identification itself.

In order to increase the accuracy of the above IOSRs, it is therefore necessary to increase p. However, from the definition of $z_{p,c}(k)$ and $z_{p,a}(k)$ it is possible to notice that their dimension grows exponentially with p. The combination of the two drawbacks is detrimental, leading to considerable computational effort, especially when the order n of the system to be identified is large. The problem becomes of paramount importance when the bilinear model to be identified is meant to approximate a more general nonlinear system, and therefore features a relatively large value of n.

In the present paper, we derive new IOSRs to overcome both the approximation issue and the curse of dimensionality. The key differences with respect to the approach taken in Reference 9 are the use of a Linear-Time-Varying (LTV) formulation of the bilinear system of Eq. (1) and an alternative application of the interaction matrices.

Time-Varying IOSRs

Any bilinear system of the form of Eq. (1) can be rewritten as a linear system with time-varying system matrix A or time-varying influence matrix B, depending on how the bilinear term $Nx(k)u(k)$ is lumped with one of the other two terms. In this work we use the time-varying system matrix formulation

$$x(k + 1) = A(k)x(k) + Bu(k) \tag{18}$$

where

$$A(k) = A + Nu(k) \tag{19}$$

TV Causal IOSRs

Propagate Eq. (18) forward in time and get

$$\begin{aligned}
x(k + 2) &= A(k + 1)x(k + 1) + Bu(k + 1) \\
&= A(k + 1)\big(A(k)x(k) + Bu(k)\big) + Bu(k + 1) \\
&= A(k + 1)A(k)x(k) + \begin{bmatrix} A(k + 1)B & B \end{bmatrix} \begin{bmatrix} u(k) \\ u(k + 1) \end{bmatrix}
\end{aligned} \tag{20}$$

From Eq. (1b), we can also write

$$\begin{aligned}
y(k + 1) &= Cx(k + 1) + Du(k + 1) \\
&= CA(k)x(k) + CBu(k) + Du(k + 1)
\end{aligned} \tag{21}$$

and put Eqs. (1b) and (21) together in matrix form

$$\begin{bmatrix} y(k) \\ y(k+1) \end{bmatrix} = \begin{bmatrix} C \\ CA(k) \end{bmatrix} x(k) + \begin{bmatrix} D & 0 \\ CB & D \end{bmatrix} \begin{bmatrix} u(k) \\ u(k+1) \end{bmatrix} \tag{22}$$

Add and subtract $M_c(k+2) \begin{bmatrix} y(k) \\ y(k+1) \end{bmatrix}$ in Eq. (20) and, plugging Eq. (22) in, obtain

$$x(k+2) = A(k+1)A(k)x(k) + \begin{bmatrix} A(k+1)B & B \end{bmatrix} \begin{bmatrix} u(k) \\ u(k+1) \end{bmatrix} + M_c(k+2) \begin{bmatrix} C \\ CA(k) \end{bmatrix} x(k)$$

$$+ M_c(k+2) \begin{bmatrix} D & 0 \\ CB & D \end{bmatrix} \begin{bmatrix} u(k) \\ u(k+1) \end{bmatrix} - M_c(k+2) \begin{bmatrix} y(k) \\ y(k+1) \end{bmatrix}$$

$$= \left(\tilde{A}_{2,c}(k+2) + M_c(k+2)\tilde{C}_{2,c}(k+2) \right) x(k) + \tilde{T}_{2,c}(k+2)\tilde{z}_{2,c}(k+2) \tag{23}$$

where

$$\tilde{A}_{2,c}(k+2) = A(k+1)A(k) \qquad \tilde{C}_{2,c}(k+2) = \begin{bmatrix} C \\ CA(k) \end{bmatrix} \qquad \tilde{z}_{2,c}(k+2) = \begin{bmatrix} u(k) \\ u(k+1) \\ y(k) \\ y(k+1) \end{bmatrix} \tag{24a}$$

$$\tilde{T}_{2,c}(k+2) = \begin{bmatrix} \begin{bmatrix} A(k+1)B & B \end{bmatrix} + M_c(k+2) \begin{bmatrix} D & 0 \\ CB & D \end{bmatrix} & -M_c(k+2) \end{bmatrix} \tag{24b}$$

and the subscript c stands for *causal*. Indeed, the superstate $z_{2,c}(k+2)$ is defined solely in terms of *past* input-output data, producing a causal representation. $M_c(k+2)$ is a time-varying interaction matrix.

For Eq. (23) to be an IOSR, the state-dependent term on the right-hand side must vanish for any $x(k)$. For a system of order $n = 2$, it is sufficient that $\tilde{C}_{2,c}(k)$ is of rank 2 at every time step k to guarantee that there exists an interaction matrix $M_c(k+2)$ such that $\tilde{A}_{2,c}(k+2) + M_c(k+2)\tilde{C}_{2,c}(k+2) = 0$. Such a condition is generally met if (A, C) is an observable pair *, which is often true in real systems, and hence the condition is much milder than Eqs. (15) or (16). This represents a crucial advantage of the resulting causal IOSR over the one presented in Reference 9, as will be discussed in the next section. Assuming $\tilde{C}_{2,c}$ is of rank 2 for every k and shifting Eq. (23) backward by 2 time steps, we can write the IOSR of order $p = 2$ as

$$x(k) = \tilde{T}_{2,c}(k)\tilde{z}_{2,c}(k) \tag{25}$$

To derive the TV causal IOSR of order p, Eq. (18) generally has to be propagated $p-1$ steps forward in time and then the following term needs to be added and subracted

$$M_c(k+p) \begin{bmatrix} y(k) \\ y(k+1) \\ ... \\ y(k+p-1) \end{bmatrix} \tag{26}$$

For $p = 3$ one obtains

$$x(k) = \left(\tilde{A}_{3,c}(k) + M_c(k)\tilde{C}_{3,c}(k) \right) x(k-3) + \tilde{T}_{3,c}(k)\tilde{z}_{3,c}(k) \tag{27}$$

---

*In some rare cases, specific values of $u(k)$ might make $(A + Nu(k), C)$ a non-observable pair even when (A, C) is an observable pair (if that occurred, the identification experiment would have to be performed again avoiding those input values); in other cases, the term $Nu(k)$ can help make $\tilde{C}$ full-rank by an appropriate choice of the input, even when (A, C) is not an observable pair.

where

$$\tilde{A}_{3,c}(k) = A(k-1)A(k-2)A(k-3) \qquad \tilde{C}_{3,c}(k) = \begin{bmatrix} C \\ CA(k-3) \\ CA(k-2)A(k-3) \end{bmatrix} \tag{28a}$$

$$\tilde{z}_{3,c}(k) = \begin{bmatrix} u(k-3) & u(k-2) & u(k-1) & y^T(k-3) & y^T(k-2) & y^T(k-1) \end{bmatrix}^T \tag{28b}$$

$$\tilde{T}_{3,c}(k) = \begin{bmatrix} A(k-1)A(k-2)B & A(k-1)B & -M_c(k) \begin{bmatrix} D & 0 & 0 \\ CB & D & 0 \\ CA(k-2)B & CB & D \end{bmatrix} \end{bmatrix} \tag{28c}$$

If $\tilde{C}_{3,c}(k)$ is of rank 3 for any k and $n \leq 3$, Eq. (27) becomes

$$x(k) = \tilde{T}_{3,c}(k)\tilde{z}_{3,c}(k) \tag{29}$$

The generalization of the TV causal IOSR for any p follows the same lines and allows us to write

$$x(k) = \left(\tilde{A}_{p,c}(k) + M_c(k)\tilde{C}_{p,c}(k)\right)x(k-p) + \tilde{T}_{p,c}(k)\tilde{z}_{p,c}(k) \tag{30}$$

which reduces to

$$x(k) = \tilde{T}_{p,c}(k)\tilde{z}_{p,c}(k) \tag{31}$$

for bilinear systems such that $\tilde{C}_{p,c}(k)$ is of rank n for any k. The superstate $\tilde{z}_{p,c}(k)$ is defined as

$$\tilde{z}_{p,c}(k) = \begin{bmatrix} u(k-p) & u(k-p+1) & \dots & u(k-1) & y^T(k-p) & y^T(k-p+1) & \dots & y^T(k-1) \end{bmatrix}^T \tag{32}$$

From Eqs. (24b) and (28c) it is very clear that the matrix relating the superstate and the state is not constant. The time dependence of the system matrix $A(k)$ makes the above IOSR matrix $\tilde{T}_{p,c}$ time-varying as well, from which the name *TV IOSR*. It is worth remarking that the interaction matrix $M_c(k)$ is time-varying because at each time step the pair $\left(\tilde{A}_{p,c}(k), \tilde{C}_{p,c}(k)\right)$ takes a different value and therefore requires a different interaction matrix to make $\tilde{A}_{p,c}(k) + M_c(k)\tilde{C}_{p,c}(k) = 0$. The time dependence of $\tilde{T}_{p,c}(k)$ is then due to both $A(k)$ and $M_c(k)$ appearing in its definition and $\tilde{T}_{p,c}(k)$ turns out to be a function of the ordered sequence $\left(u(k-p+1), u(k-p+2), ..., u(k)\right)$.

It is worth noting that when the output vector $y(k)$ has more than one entry ($q > 1$), it is generally not needed to construct the entire vector in Eq. (26) with outputs at p different time steps. The condition for Eq. (31) to hold is indeed that $\tilde{C}_{p,c}(k)$ is always of rank at least equal to n, and for a multiple-output system this can be achieved by stacking fewer than p output vectors in Eq. (26). This implies that the order p of the TV causal IOSR can be less than n for a multiple-output system. The extreme case is when n outputs are measured, making it possible to construct an exact TV causal IOSR of order as low as $p = 1$.

TV Anticausal IOSRs

The anticausal version of the TV causal IOSR can be derived in a similar fashion. Rewrite Eq. (18) as

$$x(k) = A^{-1}(k)x(k+1) - A^{-1}(k)Bu(k) \tag{33}$$

and propagate it backward by plugging

$$x(k+1) = A^{-1}(k+1)x(k+2) - A^{-1}(k+1)Bu(k+1) \tag{34}$$

into Eq. (33)

$$\begin{aligned} x(k) &= A^{-1}(k)\left(A^{-1}(k+1)x(k+2) - A^{-1}(k+1)Bu(k+1)\right) - A^{-1}(k)Bu(k) \\ &= A^{-1}(k)A^{-1}(k+1)x(k+2) - A^{-1}(k)A^{-1}(k+1)Bu(k+1) - A^{-1}(k)Bu(k) \end{aligned} \tag{35}$$

Similarly to Eq. (22), we can write (backward)

$$\begin{bmatrix} y(k+2) \\ y(k+1) \end{bmatrix} = \begin{bmatrix} C \\ CA^{-1}(k+1) \end{bmatrix} x(k+2) + \begin{bmatrix} D & 0 \\ 0 & -CA^{-1}(k+1)B + D \end{bmatrix} \begin{bmatrix} u(k+2) \\ u(k+1) \end{bmatrix} \quad (36)$$

Adding and subtracting $M_a(k) \begin{bmatrix} y(k+2) \\ y(k+1) \end{bmatrix}$ in Eq. (33) and, plugging Eq. (36) in it, get

$$\begin{aligned}
x(k) &= A^{-1}(k)A^{-1}(k+1)x(k+2) - \begin{bmatrix} A^{-1}(k)A^{-1}(k+1)B & A^{-1}(k)B \end{bmatrix} \begin{bmatrix} u(k+1) \\ u(k) \end{bmatrix} \\
&\quad + M_a(k) \begin{bmatrix} C \\ CA^{-1}(k+1) \end{bmatrix} x(k+2) + M_a(k) \begin{bmatrix} D & 0 \\ 0 & -CA^{-1}(k+1)B + D \end{bmatrix} \begin{bmatrix} u(k+2) \\ u(k+1) \end{bmatrix} \\
&\quad - M_a(k) \begin{bmatrix} y(k+2) \\ y(k+1) \end{bmatrix} \\
&= \left(\tilde{A}_{2,a}(k) + M_a(k)\tilde{C}_{2,a}(k) \right) x(k+2) + \tilde{T}_{2,a}(k)\tilde{z}_{2,a}(k) \quad (37)
\end{aligned}$$

where

$$\tilde{A}_{2,a}(k) = A^{-1}(k)A^{-1}(k+1) \qquad \tilde{C}_{2,a}(k) = \begin{bmatrix} C \\ CA^{-1}(k+1) \end{bmatrix} \qquad \tilde{z}_{2,a}(k) = \begin{bmatrix} u(k+2) \\ u(k+1) \\ u(k) \\ y(k+2) \\ y(k+1) \end{bmatrix} \quad (38a)$$

$$\tilde{T}_{2,a}(k) = \begin{bmatrix} -\begin{bmatrix} 0 & A^{-1}(k)A^{-1}(k+1)B & A^{-1}(k)B \end{bmatrix} + M_a(k) \begin{bmatrix} D & 0 & 0 \\ 0 & -CA^{-1}(k+1)B + D & 0 \end{bmatrix} & -M_a(k) \end{bmatrix} \quad (38b)$$

and the subscript a stands for *anticausal* to indicate that the superstate $\tilde{z}_{2,a}(k)$ depends only on current and future input-output data.

Again, if the first term in Eq. (37) canceled for any $x(k+2)$, a time-varying IOSR analogous to Eq. (25) would be obtained. Similar to the latter, for $n = 2$ the condition to be satisfied is that $\tilde{C}_{2,a}(k)$ is of rank 2 at every time step k.

Equation (37) refers to $p = 2$. Propagating Eq. (33) backward by $p - 1$ time steps and following the same approach as for the TV causal IOSR derivation allows us to generalize Eq. (37) to any p. We obtain

$$x(k) = \left(\tilde{A}_{p,a}(k) + M_a(k)\tilde{C}_{p,a}(k) \right)x(k+2) + \tilde{T}_{p,a}(k)\tilde{z}_{p,a}(k) \quad (39)$$

which reduces to

$$x(k) = \tilde{T}_{p,a}(k)\tilde{z}_{p,a}(k) \quad (40)$$

for bilinear systems such that $\tilde{C}_{p,a}(k)$ is of rank n for any k. The superstate $\tilde{z}_{p,a}(k)$ is defined as

$$\tilde{z}_{p,a}(k) = \begin{bmatrix} u(k+p) & u(k+p-1) & ... & u(k) & y^T(k+p) & y^T(k+p-1) & ... & y^T(k+1) \end{bmatrix}^T \quad (41)$$

Again, it is worth remarking that the IOSR matrix $\tilde{T}_{p,a}(k)$ relating the superstate and the state is not constant due to the presence of $A(k)$ and $M_a(k)$ in its definition. Additionally, the same comment made for TV causal IOSRs of multiple-output systems holds for TV anticausal IOSRs as well, allowing for exact anticausal state representations even with $p < n$.

Comparison

The TV IOSRs overcome all the above mentioned problems of the TI IOSRs, as summarized below:

1. The TV IOSRs are exact for any arbitrary bilinear system, whereas the TI IOSRs are in general approximate, although asymptotically convergent.

2. No specific bound on the input is necessary for the TV IOSRs to be exact, as opposed to the TI IOSRs.

3. The TV IOSRs are exact for minimum p ($p \leq n$).

4. The dimension of the superstate of the TV IOSRs grows linearly with p, whereas for the TI IOSRs it grows exponentially.

In particular, it is worth remarking how, beyond the obvious advantage in terms of accuracy, the dimensionality benefit is twofold for the TV IOSRs. Not only grows the state dimension slowly with p, but it is not even necessary to choose a large p.

However, in order to be able to use the TV IOSRs in the ELM or IS identification methods, the time dependence of $\tilde{T}_{p,c}$ (and $\tilde{T}_{p,a}$) must be eliminated. A form like Eq. (3), with constant T, is needed and in the next section it is shown how to transform the IOSRs of Eqs. (31) and (40) into such form.

INPUT DESIGN

As already noticed, $\tilde{T}_{p,c}(k)$ depends on the values that the ordered sequence $\big(A(k-p), A(k-p+1), ..., A(k-1)\big)$ takes. In turn, the time dependence of $A(k)$ is due to $u(k)$ only. The ordered input sequence $\big(u(k-p), u(k-p+1), ..., u(k-1)\big)$ then determines how $\tilde{T}_{p,c}(k)$ changes over time. Therefore, we can think of designing the excitation input sequence so that $\tilde{T}_{p,c}(k)$ changes in a *convenient* way. Note that the above reasoning and the analysis in this section all refer to the TV causal IOSR but they are applicable to the TV anticausal IOSR in the same exact fashion and with analogous benefit.

From time-varying to time-invariant T

The first requirement that the excitation input sequence has to satisfy is to allow us to transform the TV IOSR of Eq. (31) into the constant-T form of Eq. (3). This can be done by limiting the values that $u(k)$ can take to a finite set $U = \{u_1, u_2, ..., u_L\}$. As a consequence $A(k)$ can take L possible matrix values and therefore also the number of possible ordered sequences $\big(A(k-p), ..., A(k-1)\big)$, which uniquely determine $\tilde{T}_{p,c}(k)$, is finite. The last observation allows us to construct the following finite-dimensional extended matrix $\mathcal{T}_{p,c}$ and extended superstate $\zeta_{p,c}(k)$

$$\mathcal{T}_{p,c} = \begin{bmatrix} \tilde{T}_{p,c}^{(1)} & \tilde{T}_{p,c}^{(2)} & ... & \tilde{T}_{p,c}^{(N)} \end{bmatrix} \qquad \zeta_{p,c}(k) = \begin{bmatrix} 0 \\ ... \\ 0 \\ \tilde{z}_{p,c}(k) \\ 0 \\ ... \\ 0 \end{bmatrix} \qquad (42)$$

$\tilde{z}_{p,c}(k)$ is placed in the jth block row of $\zeta_{p,c}(k)$, where j is the index of the actual matrix value that $\tilde{T}_{p,c}$ takes at time k (among the N possible values), and all the other block rows are zeros (each block row has as many entries as the dimension of the superstate $\tilde{z}_{p,c}(k)$). The following relationship formally equal to Eq. (3) can now be written

$$x(k) = \mathcal{T}_{p,c}\zeta_{p,c}(k) \qquad (43)$$

and used to implement the ELM or IS identification methods. The same technique can be used to derive the anticausal version of the IOSR of Eq. (43)

$$x(k) = \mathcal{T}_{p,a}\zeta_{p,a}(k) \qquad (44)$$

Equations (43) and (44) are formally two time-invariant IOSRs but in this paper we continue referring to the them as TV IOSRs to emphasize that they directly stem from the time-varying IOSRs of Eqs. (31) and (40).
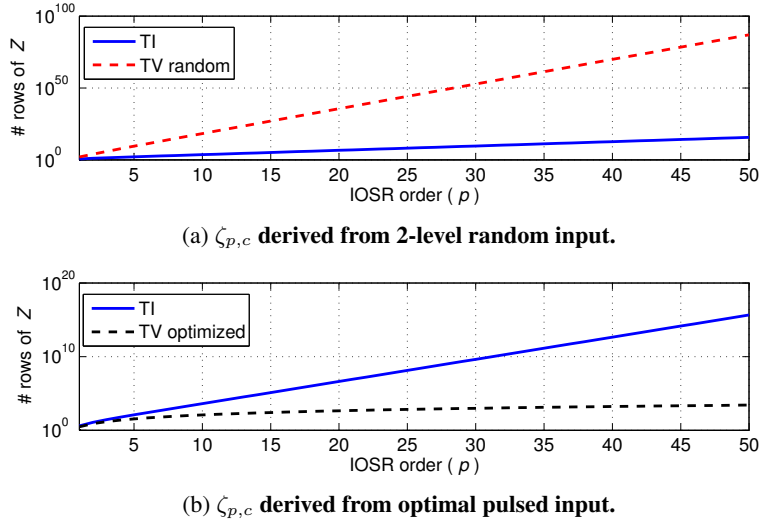
(a) $\zeta_{p,c}$ **derived from 2-level random input.**

(b) $\zeta_{p,c}$ **derived from optimal pulsed input.**

Figure 1: **Dimension increase for $z_{p,c}$ and for $\zeta_{p,c}$ for a single-output system.**

If the input value at any time step is randomly drawn from the set U, the total number of possible matrix values that $\tilde{T}_{p,c}(k)$ can take is L^p. The dimension of the extended state $\zeta_{p,c}$ is then $(q+1)pL^p$. As shown in Figure 1a, even choosing the minimum possible L (i.e. $L = 2$), the resulting growth in size of the extended superstate $\zeta_{p,c}$ is actually faster than the growth of the superstate $z_{p,c}$ of Eq. (8). Nevertheless, the exact nature of the superstate $\zeta_{p,c}$ allows the system identification engineer to select a smaller value of p with respect to the one that would be chosen if using TI IOSRs. The following example shows how the proposed algorithm indeed leads to exact identification.

Example 1. Consider the following arbitrary bilinear system from Reference 9

$$A = \begin{bmatrix} 0 & 0.5 \\ 0.5 & -0.5 \end{bmatrix} \qquad B = \begin{bmatrix} 1 \\ 2 \end{bmatrix} \qquad N = \begin{bmatrix} 0.3 & 1 \\ -1 & 1 \end{bmatrix} \qquad C = \begin{bmatrix} 0 & 1 \end{bmatrix} \qquad D = 0 \qquad (45)$$

and generate an input sequence (and the corresponding output) by randomly drawing at each time step k a value from the set $U = \{0, 0.2\}$, $k = 0, 1, ..., 1000$. Applying the ELM method based on the TV causal IOSR of Eq. (43) and the IS method based on the TV causal IOSR of Eq. (43) and the TV anticausal IOSR of Eq. (44), the results summarized in Table 1 are obtained. In all cases the identified order is correct ($n_{id} = 2$) and the output prediction error, verified on the response to a random unconstrained (i.e. $u(k)$ not restricted to take values from U only) input sequence, is close to numerical zero (10^{-14}). Notice that the identification is exact both when p is chosen to be equal to the true order n of the system and when it is assumed $p > n$ (more realistic in real applications, where the exact order of the system is not precisely known a priori). It is worth mentioning here that if 0 is not included in the allowed input levels, the input richness condition turns out not to be satisfied for the IS method and leads to an identified model of larger order (an additional step then has to be performed to reduce the model and recover the correct bilinear system matrices). It is remarkable how the proposed method can achieve very accurate identification with reduced computational effort. In Reference 9, to achieve an output prediction error of order 10^{-7} with the IS method, it was necessary to know the true order of the system ($n = 2$) and increase the order of the causal IOSR to $p = 6$, with a corresponding number of columns of 253 for R (the matrix to be decomposed by Singular Value Decomposition in the IS method, see Reference 9). When using the TV IOSRs of order $p = 2$, the same matrix R has only 36 columns and provides better identification accuracy. Additionally it is worth noting that due to the large number of zeroes in the definition of $\zeta_{p,c}$, it is generally beneficial to perform a preliminary SVD on the corresponding Z matrix to reduce its number of rows (the same applies to $\zeta_{p,a}$) and make the number of columns of R even smaller (28 in this example with $p = 2$).

11

Table 1: **Identification of the system of example 1 by random 2-level excitation.**

|	p	A eigenvalue 1	A eigenvalue 2	N eigenvalues
True	-	-0.8090169943749475	0.3090169943749474	$0.6499999999999999 \pm 0.9367496997597599i$
ELM	2	-0.8090169943749478	0.3090169943749524	$0.6499999999999947 \pm 0.9367496997597534i$
	3	-0.8090169943749496	0.3090169943749490	$0.6500000000000010 \pm 0.9367496997597594i$
	4	-0.8090169943749462	0.3090169943749483	$0.6499999999999801 \pm 0.9367496997597613i$
IS	2	-0.8090169943749470	0.3090169943749478	$0.6499999999999941 \pm 0.9367496997597653i$
	3	-0.8090169943749458	0.3090169943749453	$0.6500000000000055 \pm 0.9367496997597589i$
	4	-0.8090169943749492	0.3090169943749483	$0.6499999999999946 \pm 0.9367496997597634i$
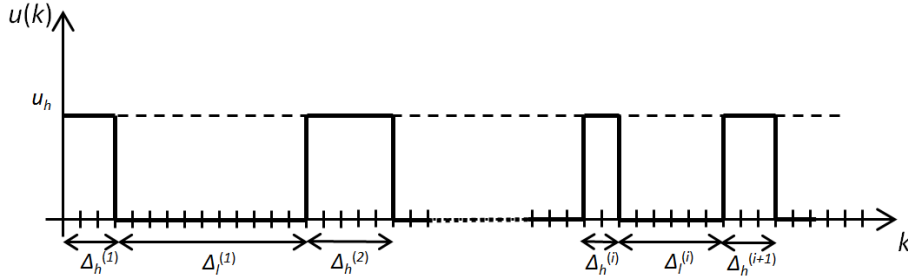
Figure 2: **Input form for optimal excitation input design.**

Input Optimization

Having proven the feasibility and correctness of the LTV approach for bilinear system identification, we now propose a technique to minimize the superstate dimension while preserving the excitation richness needed for the identification.

The chosen general form of input resembles a sequence of pulses and is shown in Figure 2, where u_h is the amplitude of the pulses, and $\Delta_h^{(i)}$ and $\Delta_l^{(i)}$ refer to the duration of the nonzero and zero input application at the ith pulse. While u_h is a fixed (constant) value, $\Delta_h^{(i)}$ and $\Delta_l^{(i)}$ are in general random discrete variables, whose possible (integer) realizations are constrained as follows

$$h_{min} \leq \Delta_h^{(i)} \leq h_{max} \tag{46}$$

$$l_{min} \leq \Delta_l^{(i)} \leq l_{max} \tag{47}$$

In other words, the excitation is a sequence of multiple pulses of fixed amplitude and different (random) duration, and its design parameters are u_h, h_{min}, h_{max}, l_{min} and l_{max}. Note that such input form satisfies the conditions established in Reference 13 for continuous-time bilinear system identifiability.

The next step consists in the choice of the input design parameters in order to minimize the dimension of $\zeta_{p,c}$. First notice from Eqs. (32) and (42) that the dimension of the superstate is $(q+1)pN$, where N is the number of combinations that any sequence $\big(u(p-k), u(p-k+1), \dots , u(k-1)\big)$ can take. With reference to Figure 2, it is then convenient to have $\Delta_l \geq p$ (i.e. fix $l_{min} \geq p$) so that each p-long input sequence embraces at most one pulse, dramatically limiting the number of possible combinations. To push the reduction of N further, one can also impose $\Delta_h = 1$ (i.e. $h_{min} = h_{max} = 1$) and get $N = p$, leaving all the variability of the pulses to the duration of the zero portions of the input sequence, i.e. Δ_l. Having fixed $l_{min} \geq p$, the only parameter to be arbitrarily chosen is then l_{max}, which does not have an impact on N. The resulting number

Table 2: Identification of the system of example 2 by multiple-pulse excitation.

	p	A eigenvalue 1	A eigenvalue 2	N eigenvalues
True	-	-0.8090169943749475	0.3090169943749474	$0.6499999999999999 \pm 0.9367496997597599i$
ELM	2	-0.8090169943749465	0.3090169943749516	$0.6499999999999837 \pm 0.9367496997597706i$
	3	-0.8090169943749496	0.3090169943749462	$0.6500000000000312 \pm 0.9367496997598526i$
	10	-0.8090169943749470	0.3090169943749515	$0.6499999993273293 \pm 0.9367497010332932i$
IS	2	-0.8090169943749468	0.3090169943749468	$0.6499999999999113 \pm 0.9367496997597923i$
	3	-0.8090169943749480	0.3090169943749460	$0.6500000000011040 \pm 0.9367496997602179i$
	10	-0.8090169943749492	0.3090169943749430	$0.6499999993267873 \pm 0.9367496981421699i$

of rows for the extended superstate $\zeta_{p,c}$ is then quadratic in p

$$n_{rows}(\zeta_{p,c}) = (q+1)(p+1)p \tag{48}$$

A closer look at Eqs. (42) and (32) suggests a further reduction can immediately be obtained, even though the growth rate remains quadratic in p. Due to the low level of the pulse sequence being zero, even the jth block row of $\zeta_{p,c}$ in Eq. (42) has some entries always equal to zero. With $\Delta_h = 1$, among all the possible j^{th} block rows of $\zeta_{p,c}$, p contain $p-1$ entries equal to 0, and one has p entries equal to 0. Hence, Eq. (48) becomes

$$n_{rows}(\zeta_{p,c}) = qp^2 + (q+1)p \tag{49}$$

Equation (49) represents the maximum number of rows that can remain after performing an initial SVD to reduce the dimension of the matrix Z constructed from the time history of $\zeta_{p,c}(k)$, which can result in an even further reduction, depending on the actual realization of the input-output sequence.

Figure 1b shows how the maximum number of rows of $\zeta_{p,c}$, Eq. (49), grows with p significantly slower when the optimized input is used. The following example also shows that the identification is still exact.

Example 2. Consider again the bilinear system of Eq. (45) and evaluate its response when subject to an input as in Figure 2 with $u_h = 0.2$, $\Delta_h = 1$, $p \leq \Delta_l \leq p+2$ ($k = 0, 1, ..., 1000$). Table 2 summarizes the results when applying the ELM method based on the TV causal IOSR of Eq. (43) and the IS method based on the TV causal IOSR of Eq. (43) and the TV anticausal IOSR of Eq. (44). In all cases the identified order is correct and the output prediction error, verified on the response to a completely random input sequence, is close to numerical zero. Notice again that the identification is exact even when the IOSR order p is chosen larger than the true system order n. It is worth mentioning that, for example, for $p = 10$ the number of rows in the *raw* matrix Z constructed from $\zeta_{p,c}$ is 220, it goes down to 120 when the all-zero rows are eliminated, and it decreases to 32 after the SVD for superspace reduction. In contrast, the number of rows of the raw Z constructed from $\zeta_{p,c}$ if the input was randomly chosen between two levels would be 20,480 and it would reach 4,194,300 if Z was built from $z_{p,c}$.

It is worth noting how the optimization of the input in order to get low-dimension IOSRs has led us to define an input sequence made of multiple pulses, similar to the one used in Reference 4. Despite using similar excitation input forms, the two identification approaches significantly differ, addressing different problems (continuous-time versus discrete-time) with different algorithms derived from different principles (more insight in the key concept underlying the present work is given in the next section). Additionally, the method presented in this paper does not necessarily need a pulsed input, although that can be computationally very beneficial when one has to rely on high-order IOSRs.

13

INTERPRETATION

The algorithms presented in this paper and in Reference 9 are based on IOSRs derived via interaction matrices. It turns out that their basic principle has an intuitive explanation in terms of state observers. As discussed in detail in Reference 14, the interaction matrices of the TI IOSRs can be interpreted as gains of an observer for the bilinear model to be identified. In the absence of noise, for *ideal* bilinear models the resulting observer is deadbeat and leads to exact IOSRs and in turn exact identification algorithms. For arbitrary bilinear systems the observer is not deadbeat but is convergent (indeed it is the fastest possible bilinear observer) and makes the identification algorithms asymptotically exact. The TV IOSRs presented in this paper can still be interpreted as state observers. More specifically, they are time-varying deadbeat observers, providing the exact estimate of the bilinear state in a finite number of steps p, i.e. only based on the values that the input and the output took over the past (in the case of causal TV IOSR) p time steps. The interaction matrix $M_c(k)$ plays then the role of a time-varying observer gain.

IDENTIFICATION OF CARLEMAN BILINEAR MODELS OF NONLINEAR SYSTEMS

This section aims to illustrate how the proposed identification algorithms can successfully be used to identify bilinear models to approximate more general nonlinear systems. Two examples are provided, Duffing's equation and Euler's equations. Being a 2$^{\text{nd}}$-order system, Duffing's equation is more meaningful than other examples in the literature of nonlinear system identification by bilinear models (Reference 4 shows examples on 1$^{\text{st}}$-order systems only). Euler's equations provide an example of greater interest in the aerospace engineering community, representing a building block of the satellite attitude dynamics. Additionally Euler's equations illustrate how the proposed identification algorithms can be applied to Multiple-Input-Multiple-Output (MIMO) systems and how for 1$^{\text{st}}$-order systems they allow one to choose the excitation input with less structure than the form in Figure 2, without incurring in computational issues.

Duffing's Equation

Duffing's equation describes the dynamics of a mass-spring oscillator with cubic spring, and is defined as

$$\ddot{y}_D(t) + c\dot{y}_D(t) + by_D^3(t) + ay_D(t) = u(t) \tag{50}$$

Equation (50) is first bilinearized by the Carleman technique to obtain a continuous-time bilinear model in the form

$$\dot{x}(t) = A_c x(t) + N_c x(t)u(t) + B_c u(t) \tag{51a}$$
$$y(t) = C_c x(t) + D_c u(t) \tag{51b}$$

which is then discretized by one of the methods presented in Reference 15 to obtain a bilinear model in the form of Eq. (1). Defining the primary state variables of Eq. (50) as

$$x_1 = y_D \qquad\qquad x_2 = \dot{y}_D \tag{52}$$

Carleman linearization (References 4,5) introduces a state vector made of progressively higher-order products of the primary state variables. For instance, the second-order Carleman state vector involves quadratic terms

$$x = \begin{bmatrix} x_1 & x_2 & x_1^2 & x_1 x_2 & x_2^2 \end{bmatrix}^T \tag{53}$$

and the third-order state vector introduces cubic terms

$$x = \begin{bmatrix} x_1 & x_2 & x_1^2 & x_1 x_2 & x_2^2 & x_1^3 & x_1^2 x_2 & x_1 x_2^2 & x_2^3 \end{bmatrix}^T \tag{54}$$

As an example, the state-space matrices of the third-order Carleman model of Duffing's equation, assuming that the only measured output is the position $x_1(t)$, are

$$A_c = \begin{bmatrix} 0 & 1 & 0 & 0 & 0 & 0 & 0 & 0 & 0 \\ -a & -c & 0 & 0 & 0 & -b & 0 & 0 & 0 \\ 0 & 0 & 0 & 2 & 0 & 0 & 0 & 0 & 0 \\ 0 & 0 & -a & -c & 1 & 0 & 0 & 0 & 0 \\ 0 & 0 & 0 & -2a & -2c & 0 & 0 & 0 & 0 \\ 0 & 0 & 0 & 0 & 0 & 0 & 3 & 0 & 0 \\ 0 & 0 & 0 & 0 & 0 & -a & -c & 2 & 0 \\ 0 & 0 & 0 & 0 & 0 & 0 & -2a & -2c & 1 \\ 0 & 0 & 0 & 0 & 0 & 0 & 0 & -3a & -3c \end{bmatrix} \tag{55a}$$

$$N_c = \begin{bmatrix} 0 & 0 & 0 & 0 & 0 & 0 & 0 & 0 & 0 \\ 0 & 0 & 0 & 0 & 0 & 0 & 0 & 0 & 0 \\ 0 & 0 & 0 & 0 & 0 & 0 & 0 & 0 & 0 \\ 1 & 0 & 0 & 0 & 0 & 0 & 0 & 0 & 0 \\ 0 & 2 & 0 & 0 & 0 & 0 & 0 & 0 & 0 \\ 0 & 0 & 0 & 0 & 0 & 0 & 0 & 0 & 0 \\ 0 & 0 & 1 & 0 & 0 & 0 & 0 & 0 & 0 \\ 0 & 0 & 0 & 2 & 0 & 0 & 0 & 0 & 0 \\ 0 & 0 & 0 & 0 & 3 & 0 & 0 & 0 & 0 \end{bmatrix} \qquad B_c = \begin{bmatrix} 0 \\ 1 \\ 0 \\ 0 \\ 0 \\ 0 \\ 0 \\ 0 \\ 0 \end{bmatrix} \tag{55b}$$

$$C_c = \begin{bmatrix} 1 & 0 & 0 & 0 & 0 & 0 & 0 & 0 & 0 \end{bmatrix} \qquad D_c = 0 \tag{55c}$$

Using Euler's discretization method (Reference 15) with step size Δt, the discrete-time bilinear model matrices are

$$A = I + A_c \Delta t \quad N = N_c \Delta t \quad B = B_c \Delta t \quad C = C_c \quad D = D_c \tag{56}$$

In order to simulate a realistic hardening spring, the Duffing coefficients in this example are chosen to be $a = c = 1$ and $b = 0.01$. The sampling time is $\Delta t = 0.002$. The objective is to identify the matrices A, N, B, C, D of Eq. (56), given input-output data. The excitation input used for identification is of the optimized type presented in Figure 2, with $u_h = 2$, $\Delta_h \in \{0.02, 0.04\}$ and $\Delta_l \in \{0.02, 0.04\}$. To verify the accuracy of the identified bilinear model, its predicted output is then compared with the output of the true system when both are driven by the same sequence of input, independent from the one used for identification. The input used for verification is shown in Figure 3, and Figure 4 shows the resulting output of the true Duffing's equation and of its bilinear approximations derived by 3rd- and 4th-order Carleman linearization and discretized by Euler's method. Figure 4 also reports the output of the linear approximation to Duffing's equation, to show how the bilinear approximation is more accurate and therefore attractive.

The condition for the TV IOSRs to be exact is that the time-varying matrices $\tilde{C}_{p,c}(k)$ and $\tilde{C}_{p,a}(k)$ have rank equal to n and given the specific structure of the matrices A and N of the Carleman model of Duffing's equation it turns out that such condition cannot be satisfied for any p. However, by looking at the structure of the 3rd-order Carleman state, Eq. (54), it is apparent how the knowledge of the primary state variable corresponding to the position (x_1) allows one to infer the higher-order state variables x_1^2 and x_1^3. It is then reasonable to feed the identification algorithm with such additional information, i.e. assuming the following output matrix

$$C = \begin{bmatrix} 1 & 0 & 0 & 0 & 0 & 0 & 0 & 0 & 0 \\ 0 & 0 & 1 & 0 & 0 & 0 & 0 & 0 & 0 \\ 0 & 0 & 0 & 0 & 0 & 1 & 0 & 0 & 0 \end{bmatrix} \tag{57}$$

With such C, the rank condition on $\tilde{C}_{p,c}(k)$ and $\tilde{C}_{p,a}(k)$ is now satisfied. Being $n = 9$ and $q = 3$, in principle $p = 3$ is sufficient for the IOSRs to be exact. However, the ratio between the largest and smallest singular values of $\tilde{C}_{3,c}(k)$ and $\tilde{C}_{3,a}(k)$ can be improved by choosing a higher value of p, e.g. $p = 10$. The 3rd-order Carleman bilinear model is identified exactly when the output is generated by the Carleman model itself, as

15

demonstrated by its extreme accuracy in predicting the output of the true Carleman model (Figure 5) when both are driven by the input of Figure 3.

The above example illustrates how the proposed algorithms are capable of identifying relatively large bilinear models ($n = 9$). However, in practice one does not know the Carleman bilinear model since the nonlinear equation itself is unknown. It is then more interesting to feed the identification algorithm with output data generated (or measured) directly from the nonlinear system and show that the algorithm is still able to find a valid bilinear model. Since in this case the data are not coming from a bilinear model but from a general nonlinear system of which a bilinear model is only an approximation, the identification algorithm operates in approximated conditions, as if there were disturbances in the input-output data. Figure 6 shows that the algorithm is able to provide an excellent bilinear approximation of Duffing's equation. In the example of Figure 6, the output data provided to the identification algorithm is the sequence formed by

$$y(k) = \begin{bmatrix} y_D(k\Delta T) & y_D^2(k\Delta T) & y_D^3(k\Delta T) & y_D^4(k\Delta T) \end{bmatrix} \tag{58}$$

and the identified bilinear model is therefore of the type of 4$^{\text{th}}$-order Carleman ($n = 14$).

It is remarkable that bilinear models of order 9 or 14 could not be identified with the algorithms presented in Ref.[9] due to the excessive computational effort required by the high dimensionality of the TI IOSRs. Another point worth mentioning is that the identification of the above Carleman models is obtained without assuming knowledge of the complete Carleman state vector, as is instead done in the examples in the literature. Reference [4] only deals with 1$^{\text{st}}$-order systems, for which it is possible to assume that all the Carleman state variables are measured, i.e. the output vector has dimension equal to n. Under such conditions, the matrices A, N and B can be identified by applying standard least-squares techniques to the state equations, and there is no need for an identification approach specialized to bilinear systems. Such extreme simplification of the bilinear identification problem when the full state is measured is reflected in the algorithms proposed in this paper by the fact that $\tilde{C}_{1,c}(k)$ and $\tilde{C}_{1,a}(k)$ would be of rank n for p as low as 1. Therefore the growth in dimension of the extended superstates $\zeta_{p,c}$ and $\zeta_{p,c}$ with p would be linear even for an unstructured input
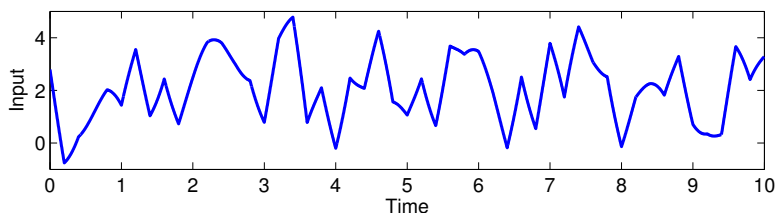

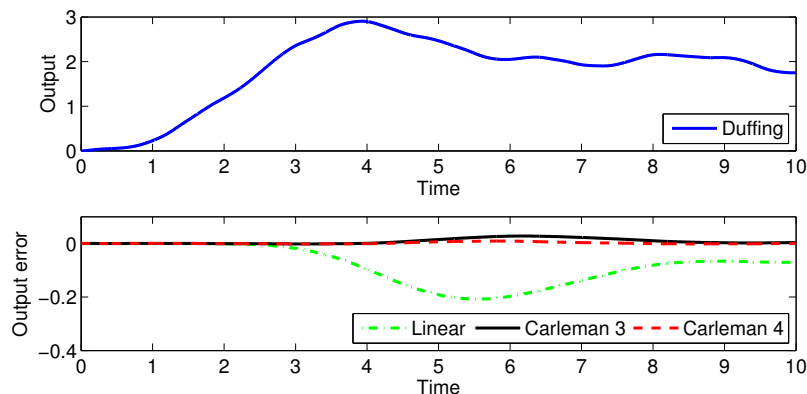**Figure 3**: **Input for the verification of the identified bilinear models.**

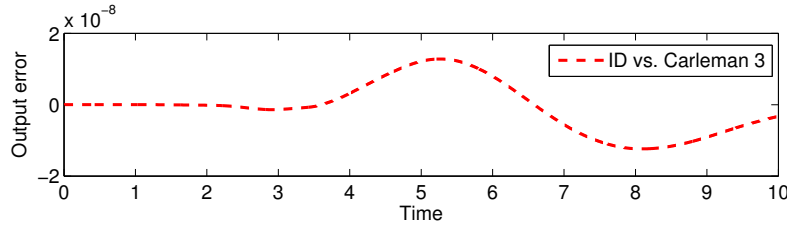 **Figure 4**: **Output of the true Duffing's equation, its linear approximation and theoretical Carleman bilinear approximations.**

Figure 5: **Prediction accuracy of the bilinear model identified from input-output data generated by the 3$^{\text{rd}}$-order theoretical Carleman bilinear model of Duffing's equation.**
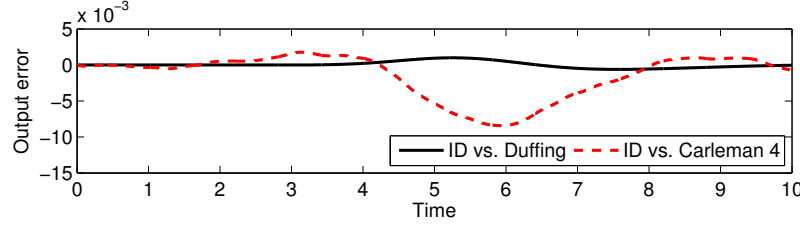

Figure 6: **Prediction accuracy of the bilinear model identified from input-output data generated by the true Duffing's equation.**

such as the one used in example 1. One can then choose a large number of allowed input levels L without incurring the curse of dimensionality, and use a completely random (quantized) input sequence. All this is illustrated by the next example.

Euler's Equations

Consider Euler's equations, which describe the rotation of a rigid body in a reference frame fixed to the rotating body and having axes coincident with the principal axes of inertia

$$
\begin{aligned}
I_1\dot{\omega}_1(t) + (I_3 - I_2)\omega_2(t)\omega_3(t) &= \tau_1(t) \\
I_2\dot{\omega}_2(t) + (I_1 - I_3)\omega_3(t)\omega_1(t) &= \tau_2(t) \\
I_3\dot{\omega}_3(t) + (I_2 - I_1)\omega_1(t)\omega_2(t) &= \tau_3(t)
\end{aligned}
\tag{59}
$$

where ω_i's are the angular velocities along the principal axes, I_i's are the principal moments of inertia and τ_i's are the applied torques, $i = 1, 2, 3$. Letting the driving torques be the sum of a feedback term $-b_i\omega_i$ and a feedforward term f_i

$$
\tau_i = -b_i\omega_i + f_i
\tag{60}
$$

and defining

$$
a_1 = \frac{I_3 - I_2}{I_1} \qquad a_2 = \frac{I_1 - I_3}{I_2} \qquad a_3 = \frac{I_2 - I_1}{I_3} \qquad c_i = \frac{b_i}{I_i} \qquad u_i = \frac{f_i}{I_i}
\tag{61}
$$

Eq. (59) becomes

$$
\begin{aligned}
\dot{\omega}_1(t) &= -a_1\omega_2(t)\omega_3(t) - c_1\omega_1(t) + u_1(t) \\
\dot{\omega}_2(t) &= -a_2\omega_3(t)\omega_1(t) - c_2\omega_2(t) + u_2(t) \\
\dot{\omega}_3(t) &= -a_3\omega_1(t)\omega_2(t) - c_3\omega_3(t) + u_3(t)
\end{aligned}
\tag{62}
$$

Defining the Carleman state as

$$
x = \begin{bmatrix} \omega_1 & \omega_2 & \omega_3 & \omega_1^2 & \omega_2^2 & \omega_3^2 & \omega_1\omega_2 & \omega_1\omega_3 & \omega_2\omega_3 \end{bmatrix}^T
\tag{63}
$$

17

a 2nd-order bilinear model is obtained

$$\dot{x}(t) = A_c x(t) + \sum_{i=1}^{3} N_{ci} x(t) u_i(t) + B_c u(t) \tag{64a}$$

$$y(t) = C_c x(t) + D_c u(t) \tag{64b}$$

where

$$A_c = - \begin{bmatrix} c_1 & 0 & 0 & 0 & 0 & 0 & 0 & 0 & a_1 \\ 0 & c_2 & 0 & 0 & 0 & 0 & 0 & a_2 & 0 \\ 0 & 0 & c_3 & 0 & 0 & 0 & a_3 & 0 & 0 \\ 0 & 0 & 0 & 2c_1 & 0 & 0 & 0 & 0 & 0 \\ 0 & 0 & 0 & 0 & 2c_2 & 0 & 0 & 0 & 0 \\ 0 & 0 & 0 & 0 & 0 & 2c_3 & 0 & 0 & 0 \\ 0 & 0 & 0 & 0 & 0 & 0 & c_1+c_2 & 0 & 0 \\ 0 & 0 & 0 & 0 & 0 & 0 & 0 & c_1+c_3 & 0 \\ 0 & 0 & 0 & 0 & 0 & 0 & 0 & 0 & c_2+c_3 \end{bmatrix} \tag{65a}$$

$$B_c = \begin{bmatrix} 1 & 0 & 0 \\ 0 & 1 & 0 \\ 0 & 0 & 1 \\ 0 & 0 & 0 \\ 0 & 0 & 0 \\ 0 & 0 & 0 \\ 0 & 0 & 0 \\ 0 & 0 & 0 \\ 0 & 0 & 0 \end{bmatrix} \quad N_{c1} = \begin{bmatrix} 0 & 0 & 0 & 0 & 0 & 0 & 0 & 0 & 0 \\ 0 & 0 & 0 & 0 & 0 & 0 & 0 & 0 & 0 \\ 0 & 0 & 0 & 0 & 0 & 0 & 0 & 0 & 0 \\ 2 & 0 & 0 & 0 & 0 & 0 & 0 & 0 & 0 \\ 0 & 0 & 0 & 0 & 0 & 0 & 0 & 0 & 0 \\ 0 & 0 & 0 & 0 & 0 & 0 & 0 & 0 & 0 \\ 0 & 1 & 0 & 0 & 0 & 0 & 0 & 0 & 0 \\ 0 & 0 & 1 & 0 & 0 & 0 & 0 & 0 & 0 \\ 0 & 0 & 0 & 0 & 0 & 0 & 0 & 0 & 0 \end{bmatrix} \tag{65b}$$

$$N_{c2} = \begin{bmatrix} 0 & 0 & 0 & 0 & 0 & 0 & 0 & 0 & 0 \\ 0 & 0 & 0 & 0 & 0 & 0 & 0 & 0 & 0 \\ 0 & 0 & 0 & 0 & 0 & 0 & 0 & 0 & 0 \\ 0 & 0 & 0 & 0 & 0 & 0 & 0 & 0 & 0 \\ 0 & 2 & 0 & 0 & 0 & 0 & 0 & 0 & 0 \\ 0 & 0 & 0 & 0 & 0 & 0 & 0 & 0 & 0 \\ 1 & 0 & 0 & 0 & 0 & 0 & 0 & 0 & 0 \\ 0 & 0 & 0 & 0 & 0 & 0 & 0 & 0 & 0 \\ 0 & 0 & 1 & 0 & 0 & 0 & 0 & 0 & 0 \end{bmatrix} \quad N_{c3} = \begin{bmatrix} 0 & 0 & 0 & 0 & 0 & 0 & 0 & 0 & 0 \\ 0 & 0 & 0 & 0 & 0 & 0 & 0 & 0 & 0 \\ 0 & 0 & 0 & 0 & 0 & 0 & 0 & 0 & 0 \\ 0 & 0 & 0 & 0 & 0 & 0 & 0 & 0 & 0 \\ 0 & 0 & 0 & 0 & 0 & 0 & 0 & 0 & 0 \\ 0 & 0 & 2 & 0 & 0 & 0 & 0 & 0 & 0 \\ 0 & 0 & 0 & 0 & 0 & 0 & 0 & 0 & 0 \\ 1 & 0 & 0 & 0 & 0 & 0 & 0 & 0 & 0 \\ 0 & 1 & 0 & 0 & 0 & 0 & 0 & 0 & 0 \end{bmatrix} \tag{65c}$$

$$C_c = \begin{bmatrix} 1 & 0 & 0 & 0 & 0 & 0 & 0 & 0 & 0 \\ 0 & 1 & 0 & 0 & 0 & 0 & 0 & 0 & 0 \\ 0 & 0 & 1 & 0 & 0 & 0 & 0 & 0 & 0 \end{bmatrix} \quad D_c = \begin{bmatrix} 0 & 0 & 0 \\ 0 & 0 & 0 \\ 0 & 0 & 0 \end{bmatrix} \tag{65d}$$

By Eq. (56) the following discrete-time model with 3 inputs is obtained

$$x(k+1) = A x(k) + \sum_{i=1}^{3} N_i x(k) u_i(k) + B u(k) \tag{66a}$$

$$y(k) = C x(k) + D u(k) \tag{66b}$$

The excitation input of Figure 7 generates the output history $\omega_1(t)$, $\omega_2(t)$, $\omega_3(t)$ in accordance with Eq. (62) assuming $I_1 = 30$, $I_2 = 20$, $I_3 = 10$, $b_1 = b_2 = b_3 = 3$ and sampling with $\Delta t = 0.002s$. Note that following the same reasoning as for the example of Duffing's equation, the output data fed to the identification algorithm is

$$y(k) = \begin{bmatrix} \omega_1(k) & \omega_2(k) & \omega_3(k) & \omega_1^2(k) & \omega_2^2(k) & \omega_3^2(k) & \omega_1(k)\omega_2(k) & \omega_1(k)\omega_3(k) & \omega_2(k)\omega_3(k) \end{bmatrix}^T \tag{67}$$
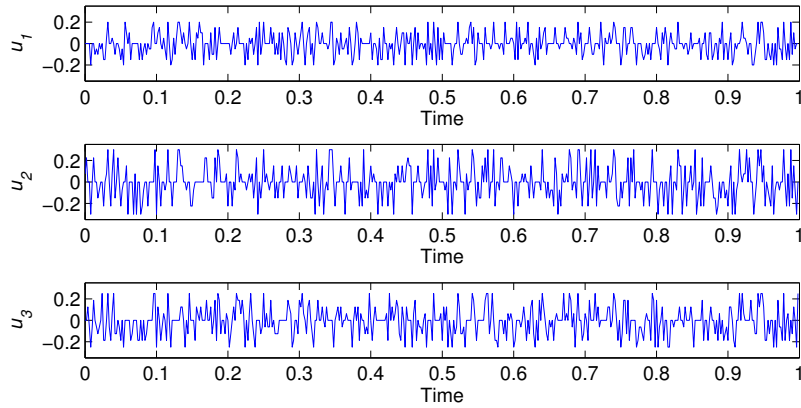
Figure 7: **Excitation input for the identification of Euler's equations.**
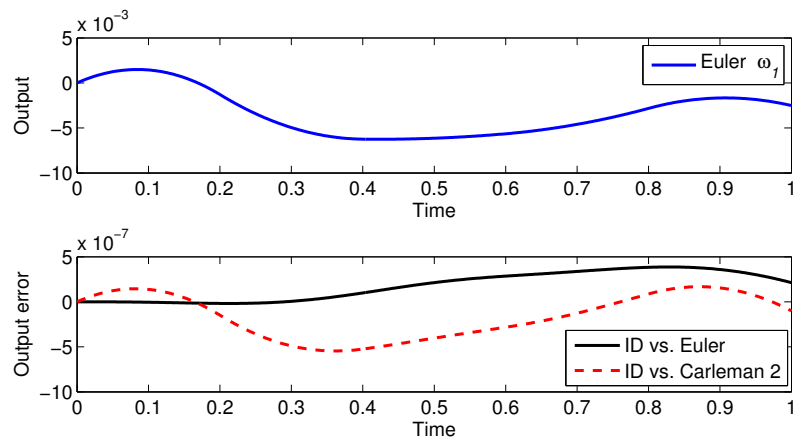

Figure 8: $\omega_1(t)$ **of the true Euler's equations and comparison with its theoretical and identified 2ⁿᵈ-order Carleman bilinear approximation.**

i.e. the number of measured outputs from the point of view of the Carleman model to be identified is $q = n$ and p can be set to a value less than n, in this example $p = 1$. This allows us to choose a less structured input, possibly simpler to implement in some applications, without incurring in computational issues.

The identified bilinear model has the correct order $n_{id} = 9$ and accurately predicts the output of both the true Euler equations and their Carleman approximation of 2ⁿᵈ order. For verification, all the three models are driven by an input sequence independently generated from the one used for identification and as an example the comparison of their output ω_1 is shown in Figure 8.

CONCLUSION

This paper has extended the family of Input-Output-to-State Representations (IOSRs) for bilinear systems, i.e. relationships expressing the bilinear state as a linear combination of input-output data only. The new IOSRs feature crucial benefits over the ones presented in Reference 9. In particular they are exact for any arbitrary bilinear system satisfying minimum observability conditions, and without imposing restrictions on the magnitude that the excitation input can take. These characteristics have been obtained by exploiting the linear-time-varying nature of bilinear systems and by designing an optimal excitation input form in terms

of richness and reduced complexity. The resulting algorithms can be applied to identify systems which are inherently bilinear (Reference 1) as well as bilinear models approximating more general nonlinear systems (Reference 4). Numerical examples have been given for both cases, showing how the approach offers benefits over existing methods. In particular, the identification algorithms are exact for arbitrary bilinear systems and the computational effort is sufficiently reduced to allow one to identify relatively large bilinear models. For these reasons, the proposed approach to bilinear discrete-time system identification can play an important role in the identification of high-order bilinear models, as is typically the case when using bilinear models as a bridge between linear and nonlinear systems. The examples of Duffing's equation and Euler's equations have illustrated how the identification method can be used to find bilinear models approximating more general nonlinear systems without going through the tedious process of Carleman linearization. The method can also be applied directly to the identification of unknown nonlinear systems, whose input-output data only are known (from measurements).

Although the proposed method has been proven to achieve the exact identification of high-dimensional models arising from Carleman linearization of nonlinear systems, further research will focus on how to reduce the order of the identified bilinear models and on how to explicitly and optimally take into account the inevitable noise in the experimental input-output data in the formulation of the discrete-time bilinear system identification algorithms.

REFERENCES

[1] C. Bruni, G. Di Pillo, and G. Koch, "On the Mathematical Models of Bilinear Systems," *Ricerche di Automatica*, Vol. 2, No. 1, 1971, pp. 11–26.

[2] S. Svoronos, G. Stephanopoulos, and A. Rutherford, "Bilinear Approximation of General Non-Linear Dynamic Systems with Linear Inputs," *International Journal of Control*, Vol. 31, No. 1, 1980, pp. 109–126.

[3] J. T.-H. Lo, "Global Bilinearization of Systems with Control Appearing Linearly," *SIAM Journal on Control*, Vol. 13, No. 4, 1975, pp. 879–885.

[4] C.-H. Lee and J.-N. Juang, "Nonlinear System Identification - A Continuous-Time Bilinear State Space Approach," *Advances in the Astronautical Sciences*, Vol. 139, 2011, pp. 421–444.

[5] K. Kowalski and W.-H. Steeb, *Nonlinear Dynamical Systems and Carleman Linearization*. Singapore: World Scientific, 1991.

[6] J. Minisini, A. Rauh, and E. P. Hofer, "Carleman Linearization for Approximate Solutions of Nonlinear Control Problems: Part 1 - Theory," *Advances in Mechanics, Dynamics and Control; Proceedings of the 14th International Workshop on Dynamics and Controls*, Moskov, 2007.

[7] A. Rauh, J. Minisini, and E. P. Hofer, "Carleman Linearization for Approximate Solutions of Nonlinear Control Problems: Part 2 - Applications," *Advances in Mechanics, Dynamics and Control; Proceedings of the 14th International Workshop on Dynamics and Controls*, Moscow, 2007.

[8] M. Q. Phan and H. Celik, "A Superspace Method for Discrete-Time Bilinear Model Identification by Interaction Matrices," *Advances in the Astronautical Sciences*, Vol. 139, 2011, pp. 445–464.

[9] F. Vicario, M. Q. Phan, R. Betti, and R. W. Longman, "Linear State Representations for Identification of Bilinear Discrete-Time Models by Interaction Matrices," *Advances in the Astronautical Sciences*, Vol. 148, 2013, pp. 2039–2058.

[10] J.-N. Juang, M. Q. Phan, L. G. Horta, and R. W. Longman, "Identification of Observer/Kalman Filter Markov Parameters: Theory and Experiments," *Journal of Guidance, Control, and Dynamics*, Vol. 16, No. 2, 1993, pp. 320–329.

[11] M. Q. Phan, "Interaction Matrices in System Identification and Control," *Proceedings of the15th Yale Workshop on Adaptive and Learning Systems*, New Haven, CT, 2011.

[12] N. Berk Hizir, M. Q. Phan, R. Betti, and R. W. Longman, "Identification of discrete-time bilinear systems through equivalent linear models," *Nonlinear Dynamics*, Vol. 69, No. 4, 2012, pp. 2065–2078.

[13] E. Sontag, Y. Wang, and A. Megretski, "Input Classes for Identifiability of Bilinear Systems," *IEEE Transactions on Automatic Control*, Vol. 54, No. 2, 2009, pp. 195–207.

[14] M. Q. Phan, F. Vicario, R. Betti, and R. W. Longman, "Observers for Bilinear State-Space Models by Interaction Matrices," *Proceedings of the16th Yale Workshop on Adaptive and Learning Systems*, New Haven, CT, 2013.

[15] M. Q. Phan, Y. Shi, R. Betti, and R. W. Longman, "Discrete-Time Bilinear Representation of Continuous-Time Bilinear State-Space Models," *Advances in the Astronautical Sciences*, Vol. 143, 2012, pp. 571–589.